

The Formation of Dimensionally Ordered Silicon Nanowires within Mesoporous Silica

Nicholas R. B. Coleman,[†] M. A. Morris,^{†,‡}
Trevor R. Spalding,[†] and Justin D. Holmes^{*,†,‡}

Department of Chemistry and Supercritical Fluid Centre
University College Cork, Cork, Ireland

Received September 11, 2000

Nanoscale one-dimensional (1D) structures of semiconductor nanowires are expected to play a vital role as materials for both interconnects and emerging future technologies because of their low-dimensionality and unique optical, electrical, and mechanical properties.¹ Even though the preparation of semiconductor nanowires in bulk quantities is now possible, unanswered questions relating to their processibility remain: namely, how can they be evenly distributed across a surface, or within a 3 D structure, and how can they be made sufficiently robust to be used practically within planar or multidimensional devices? Consequently, a limiting step toward the development of nanotechnologies is the configuration of nanowires into useful electronic device architectures.² Recently, mesoporous solids³ that contain uni-directional arrays of pores, typically 2–15 nm in diameter, running throughout the material have been exploited as templates for semiconductor materials formed from the gas phase.^{4–6} Certainly, these gas-phase methods have yielded high-quality semiconductor nanomaterials but very often high temperatures or extensive reaction times are required for successful nucleation and growth of the materials within the mesopores making these techniques often costly and time-consuming.^{4,6} In this communication we describe the use of a novel supercritical fluid solution-phase technique to rapidly fill the pores of mesoporous silica with silicon nanowires. The silica mesoporous matrix provides a means of producing a high density of stable, well-ordered arrays of semiconductor nanowires.

Hexagonal mesoporous silica was prepared by hydrolyzing tetramethoxysilane (TMOS) in the presence of a poly(ethylene oxide) (PEO)–poly(propylene oxide) (PPO) triblock copolymer surfactant (PEO₂₆PPO₃₉PEO₂₆) and HCl (0.5 M).⁷ Silicon nanowires were formed within the pores of the mesoporous silica by degrading diphenylsilane (0.022 mol in hexane) in a high-pressure

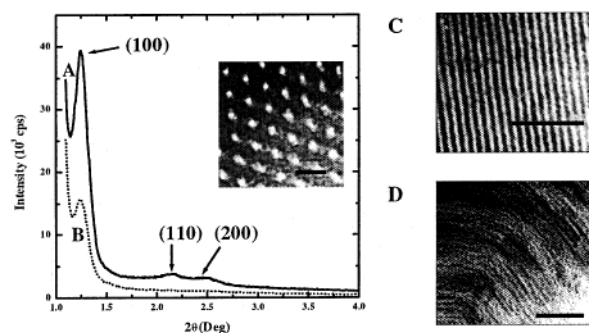


Figure 1. PXRD patterns of (a) as-synthesized calcined mesoporous silica prepared by using the PEO₂₆PPO₃₉PEO₂₆ triblock copolymer surfactant and (b) the same hexagonal mesoporous sample after silicon nanowire inclusion in the mesopores. The insert shows the ordered arrays of pores in the mesoporous matrix (scale bar = 12 nm). “Side-on” TEM image of (c) the as-synthesized calcined mesoporous silica (scale bar = 50 nm) and (d) after incorporation of silicon through diphenylsilane decomposition (scale bar = 50 nm).

reaction cell at 500 °C and a pressure of 375 bar for 15 min.⁸ The white mesoporous materials changed color from white to yellow to dark orange/red during the course of the reaction. The end product was homogeneous in appearance. No color change was observed in the absence of diphenylsilane. After the reaction had finished, the contents of the cell were washed with hexane and the relatively large (~1 mm dimensions) particles of the dark orange/red mesoporous silica incorporating silicon were manually extracted and dried for analysis.⁹

Figure 1a shows the powder X-ray diffraction (PXRD) pattern of the calcined mesoporous silica used in the present work. Three well-resolved peaks can be readily indexed to (100), (110), and (200) reflections for a hexagonal mesoporous solid.^{3,10} The position of the intense (100) peak reflects a *d* spacing of 7.1 nm corresponding to a pore-to-pore distance of 8.2 nm. Complementary to the PXRD data, transmission electron microscopy (TEM) revealed that the calcined mesoporous silica had a well-ordered mesoscopic structure with a wall thickness and pore diameter of approximately 3 and 5 nm, respectively. A pore-to-pore distance of 8.3 nm was obtained by low-angle PXRD after inclusion of silicon in the mesoporous silica (Figure 1b). The reduced intensity

(8) The cell was attached, via a three-way valve, to a stainless steel high-pressure tube (~21 mL) equipped with a stainless steel piston. An Isco high-pressure pump (Isco Instruments, PA) was used to pump CO₂ into the back of the piston and displace oxygen-free anhydrous hexane into the reaction cell to 375 bar.¹⁶ The cell was placed in a furnace and heated to 500 °C (±1 °C) using a platinum resistance thermometer and temperature controller. The reaction proceeded at these conditions for 15 min. The high pressures and temperatures used in these experiments and the volatile nature of the chemicals could potentially lead to fire or explosion. Suitable safety precautions should be taken into consideration including the use of a blast screen.

(9) A JEOL 1200 EX electron microscope operating with an 80 kV accelerating voltage was used for transmission electron microscopy (TEM). Samples were redispersed in chloroform and a drop of the mixture was placed on a carbon-coated copper TEM grid. Powder X-ray diffraction (PXRD) profiles were recorded on a Philips 3710 PWD diffractometer, equipped with a Cu K α radiation source and standard scintillation detector. Silicon magic angle spinning nuclear magnetic resonance (²⁹Si MAS NMR) spectra were obtained at room temperature using a Chemagnetics CMX Lite 300 MHz apparatus. Pulses of 30° with 4 s pulse width were used. Pulse delay times were varied in the range 60 to 10 000 s depending on the relaxation process. Samples were spun at 5 kHz. Chemical shifts are quoted relative to tetramethylsilane and referenced using tetramethoxysilane. The UV–visible spectra of the silica samples suspended in ethanol were recorded on a Hewlett-Packard HP 8543 diode array spectrophotometer. The surface areas of the samples were measured using nitrogen BET isotherms at 77 K on a Micromeritics ASAP 2010 volumetric analyser (Norcross, GA). Before the adsorption data were taken the samples were degassed for 12 h at 120 °C.

(10) Junges, U.; Jacobs, W.; Voigt-Martin, I.; Krutzsch, B.; Schuth, F. *J. Chem. Soc., Chem. Commun.* **1995**, 2283. Zhao, D.; Sun, J.; Li, Q.; Stucky, G. D. *Chem. Mater.* **2000**, *12*, 275.

* To whom correspondence should be addressed: Tel: +353 (0)21 4903608. Fax: +353 (0)21 4274097. E-mail: j.holmes@ucc.ie.

[†] Department of Chemistry.

[‡] Supercritical Fluid Centre.

(1) Brus, L. *J. Phys. Chem.* **1994**, *98*, 3575. Yeh, C.-Y.; Zhang, S. B.; Zunger, A. *Phys. Rev. B* **1994**, *50*, 14405.

(2) Li, Y.; Xu, D.; Zhang, Q.; Chen, D.; Huang, F.; Xu, Y.; Guo, G.; Gu, Z. *Chem. Mater.* **1999**, *11*, 3433. Schmid, G.; Baumle, M.; Geerkens, M.; Heim, I.; Osemann, C.; Sawitowski, T. *Chem. Soc. Rev.* **1999**, *28*, 179. Nguyen, P. P.; Pearson, D. H.; Tonucci, R. J.; Babcock, K. *J. Electrochem. Soc.* **1998**, *145*, 247.

(3) Kresage, C. T.; Leonwicz, M. E.; Roth, W. J.; Vartuli, J. C.; Beck, J. S. *Nature* **1992**, *359*, 710. Yu, C.; Yu, Y.; Zhao, D. *Chem. Commun.* **2000**, 575. Schmidt-Winkel, P.; Glinka, C. J.; Stucky, G. D. *Langmuir* **2000**, *16*, 356. Whitehead, A. H.; Elliott, J. M.; Owen, J. R.; Attard, G. S. *Chem. Commun.* **1999**, 331.

(4) Leon, R.; Margolese, D.; Stucky, G.; Petroff, P. M. *Phys. Rev. B* **1995**, *52*, R2285.

(5) Moller, K.; Bein, T. *Chem. Mater.* **1998**, *10*, 2950.

(6) Dag, O.; Ozin, G. A.; Yang, H.; Reber, C.; Bussiere, G. *Adv. Mater.* **1999**, *11*, 474.

(7) The synthesis of mesoporous silica is based on a method described by Attard et al. (*Nature*, **1995**, 378, 366). Synperonic PE/P85 (1 g) was dissolved in TMOS (1.8 g) and added to a solution of HCl (1 g, 0.5 M HCl). Methanol generated during the reaction was removed on a rotary evaporator at 40 °C. The resulting viscous gel was left to condense at 40 °C for one week in a sealed flask. Calcination of the silica was carried out in air for 24 h at 450 °C.

of the (100) peak and the absence of (110) and (200) peaks noted after silylation probably arises from the inclusion of silicon in the mesopores, possibly resulting in an increased residual strain on the silica walls.¹¹

The TEM images shown in parts c and d of Figure 1 are evidence for inclusion of silicon in the mesopores. Figure 1c displays a “side-on” view of the mesoporous matrix showing good contrast between the silica walls and the empty pores. A side-on view of mesoporous silica incorporating crystalline silicon shows very little contrast between the silica walls and the silicon. This is expected since the work functions of SiO₂ and Si are similar. A comparison of these two TEM images (Figure 1c,d) is consistent with silicon filling the mesopores. We believe that such a comprehensive filling of the pores with semiconductor nanowires has not previously been observed using other inclusion methods. Moreover, the comparatively short reaction time of the present method makes it noteworthy. At diphenylsilane concentrations above 0.002 mol “whiskers” of silicon wires several microns in length (not shown) were observed to extrude from the mesoporous surface. Hence, the mesopores appear to act as directional templates for surface nanowire growth once the pores have been filled. The purity and crystallinity of the mesoporous silicon nanowires was confirmed by PXRD at high angles. The relatively sharp peaks in the PXRD pattern can be indexed to a diamond structure of silicon with a lattice constant $a = 0.357$ nm, which is in good agreement with literature values for silicon.¹²

Silicon magic angle spinning nuclear magnetic resonance (²⁹Si MAS NMR) was undertaken on a mesoporous silica sample before and after silicon inclusion. As synthesized, the mesoporous silica displays two distinct ²⁹Si chemical shifts at -103.4 and -111.4 ppm respectively assigned to species Q₃(SiO₃(OH)) and Q₄(SiO₄).^{6,13} A smaller feature apparent at -92.4 ppm was assigned to Q₂(SiO₂(OH)₂).⁶ The Q₃ and Q₂ peaks result predominantly from species at the surface of the silica walls of each pore whereas Q₄ species are within the bulk silica walls. The Q₄ to (Q₃ + Q₂) peak area ratio of 0.5 is consistent with a wall thickness that is approximately 0.33–0.5 times the size of the pore diameter¹³ and is complementary to the results obtained by PXRD and TEM. New peaks centered around -80 ppm and a complete loss in the intensity of the Q₃ peak at -103.4 ppm were observed upon inclusion of silicon in the pores. Curve fitting of the peak at -80 ppm resolved two features, a relatively sharp peak at approximately -80.8 ppm and a broader less distinct peak at -88.0 ppm. The peak at -80.8 ppm is most probably due to crystalline silicon (Si₄Si) as, in a control experiment, silicon from a powdered Si(111) wafer produced a single sharp peak at -82.5 ppm. The small downfield shift of -1.7 ppm (relative to the powdered wafer) most likely results from the lattice expansion of the SiO₂ walls after silicon inclusion resulting in lower electron densities. We have assigned the peak at -88.0 ppm to silicon atoms attached at the surface of the intrachannel silicon (Si₃(wall)-O-Si(wire)). The loss of surface Si-OH site resonances at -103.4 (Q₃(SiO₃(OH))) and -92.4 ppm (SiO₂(OH)₂) and the formation of the Si₃(wall)-O-Si(wire) peak probably infers that the silicon nanowires are anchored to the surface of the mesoporous walls and pore-filling has been achieved. ²⁹Si MAS NMR also revealed that the volume ratio of silicon to silica in the mesoporous sample was ~29%, which correlates to ~80% of the mesopores being filled with silicon.

(11) Marler, B.; Oberhagemann, U.; Vortmann, S.; Gies, H. *Microporous Mater.* **1996**, *6*, 375.

(12) JCPDS International Centre for Diffraction Data; Powder Diffraction file 27-1402; 0.357 nm: 1984.

(13) Steel, A.; Carr, S. W.; Anderson, M. W. *Chem. Mater.* **1995**, *7*, 1829.

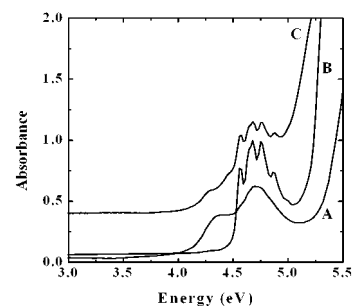


Figure 2. UV-visible absorbance spectrum of (a) as-synthesized calcined mesoporous silica mesoporous, (b) silicon nanowires grown from gold nanocrystals, and (c) silica loaded with crystalline silicon nanowires.

Nitrogen absorption-desorption isotherms obtained for a calcined mesoporous silica sample exhibited a high surface area of ~1045 m² g⁻¹. Upon inclusion of the silicon nanowires in the mesopores the surface area decreased to ~72 m² g⁻¹, which supports the hypothesis that the pores have been filled.

Figure 2 shows the UV-visible absorption of as-synthesized calcined mesoporous silica before (Figure 3a) and after incorporation of crystalline silicon (Figure 3c) and also the electronic spectrum of micron length silicon nanowires (Figure 3b), ~4 nm in diameter, grown using colloidal gold nanoparticles as nucleation seeds.¹⁴ The mesoporous silicon nanowires possess similar optical properties to the silicon nanowires seeded from the gold nanocrystals. Both samples show a strongly blue-shifted absorption band-edge from the bulk indirect gap of 1.1 eV and display sharp, discrete absorbance features. It is likely that these optical properties result from quantum confinement effects.¹⁵ Both the mesoporous silicon and Au-grown silicon nanowire samples exhibit strong absorption features centered at 4.7 eV indicative of the L → L transition previously reported for (100) orientated silicon nanowires.¹⁴ Additional peaks in the mesoporous silicon sample that are not observed in the Au-grown silicon nanowires are centered at 4.25 eV probably arise from absorption due to the silica mesoporous solid. The UV-visible spectra confirm that the mesoporous silicon nanowires possibly exhibit quantum confinement effects previously observed in colloidal grown nanowires.

In conclusion, a novel supercritical fluid solution phase technique has been utilized to fill 5 nm diameter pores of hexagonal mesoporous silica with quantum-confined silicon nanowires. This is the first example of utilizing supercritical fluids as an inclusion medium for mesoporous materials. The high diffusivity¹⁶ of the supercritical fluid phase, of the order of 10⁻³–10⁻⁴ cm² s⁻¹, enables rapid diffusion of reactant precursor into the pores of the silica matrix where swift nucleation and growth can occur resulting in a reaction rate several orders of magnitude faster than are obtainable using traditional gas-phase or solution-phase deposition methods.

Acknowledgment. The authors acknowledge financial support from HEA Ireland, Enterprise Ireland, and Intel (Ireland). The authors are grateful to Dr W. J Reville for Electron Microscopy Support at UCC.

JA005598P

(14) Gold-grown nanowires were prepared using a modification of the method published by Holmes et al. (*Science*, **2000**, *287*, 1471). Under a nitrogen atmosphere, dodecanethiol-capped gold nanocrystals were dispersed in diphenylsilane with a Au:Si ratio of 0.1%, then loaded into the high-pressure cell (5 mL) and sealed under a nitrogen atmosphere. The cell was heated and pressurized as previously described.⁸

(15) Hu, J.; Odom, T. W.; Lieber, C. M. *Acc. Chem. Res.* **1999**, *32*, 435.

(16) Clifford, T. *Fundamentals of Supercritical Fluids*, 1st ed.; Oxford University Press: New York, 1998.